An efficient salp swarm-inspired algorithm for parameters identification of photovoltaic cell models

Rabeh Abbassi[a,b,c,*], Abdelkader Abbassi[a], Ali Asghar Heidari[d], Seyedali Mirjalili[e]

[a] *University of Kairouan, Institute of Applied Sciences and Technology of Kasserine (ISSATKas), PO Box 471, 1200 Kasserine, Tunisia*
[b] *University of Hail, College of Engineering, Saudi Arabia*
[c] *University of Tunis, Higher National Engineering School of Tunis (ENSIT), LaTICE Laboratory, 5 Avenue Taha Hussein, PO Box 56, 1008 Tunis, Tunisia*
[d] *School of Surveying and Geospatial Engineering, University of Tehran, Tehran, Iran*
[e] *Institute of Integrated and Intelligent Systems, Griffith University, Nathan, Brisbane, QLD 4111, Australia*

ABSTRACT

Solar Photovoltaic systems (SPVSs) are becoming one of the most popular renewable energy technology for generating significant share of electric power. With the consistent growth of SPVSs applications, the challenge of parameters estimation of photovoltaic cells has drawn the attention of researchers and industrialists and gained immense momentum for SPVSs modeling. This paper proposes an efficient approach based on Salp Swarm Algorithm (SSA) for extracting the parameters of the electrical equivalent circuit of PV cell based double-diode model. The experimental and comparative results demonstrate that SSA is highly competitive with the results of two algorithms that have never been used before for the PV cell parameter extraction namely Sine Cosine Algorithm (SCA) and Virus Colony Search Algorithm (VCS). SSA is also significantly better than three well-established parameter extraction algorithms namely Ant Lion Optimizer (ALO), Gravitational Search Algorithm (GSA) and Whale Optimization Algorithm (WOA). Several evaluation criteria including Mean Square Error (MSE), Absolute Error (AE) and statistical criterion show that the SSA algorithm provides the highest value of accuracy and has merits in designing SPVSs.

1. Introduction

Nowadays, the priority given to alternative energy sources is boosted strongly to address several critical issues [1]. The problems in question are essentially the energy crisis, the exhaustion of fuels, the pollution of the environment, and climate change [2]. Solar or photovoltaic (PV) energy is a renewable energy source that respects the ecological balance and promotes the sustainable development [3]. Photovoltaic systems (PVSs) are static mediums that are used for the direct conversion of solar energy into electricity. Before the installation of a PVS, the prediction of its performance depends on a reliable model design estimating the equivalent circuit DC parameters. The accuracy of such an estimation is very important for many purposes, which depends on the number of DC parameters presented in that model. Indeed, it is very useful for the extraction of DC PV cell parameters and understanding their impact on the model efficiency as well as the optimization of the fabrication processes [4,2]. However, it is unfortunate that the manufacturers often provide insufficient information in the data sheets, which is required to accurately simulate the characteristics of a PVS, especially under diverse environmental conditions [5]. To overcome these challenges, several works investigated the use of nonlinear electrical models of solar cells to extract its effective parameters [6–8]. As for any physical system, the PV cell modeling is always done with different levels of accuracy, depending on the users purposes. This task is consistently achieved through an equivalent circuit and by using concentrated parameters and variables [2]. Herein, it is of a paramount importance to mention that the most imperative parameters of the PV cells or modules are extracted based on several mathematical models, which simulate their behavior under various operating conditions.

Among variety of the existing models in literature, the noteworthy models are: Single-Diode Model (SDM) [6], Double- Diode Model (DDM) [9] and Three-Diode Model (TDM) [2]. Apart from these detailed models, the other ones, which are less itemized in literature, are a single-diode model with parasitic capacitor [10], improved two-diode model [11,12], reverse two-diode model, generalized three-diode model [13], diffusion based model [14], and multi-diode model [15].

* Corresponding author.
E-mail addresses: r_abbassi@yahoo.fr (R. Abbassi), abd_abbassi@yahoo.com (A. Abbassi), as_heidari@ut.ac.ir (A.A. Heidari), seyedali.mirjalili@griffithuni.edu.au (S. Mirjalili).

Among various models, the SDM is considered as a reference model and it is the most commonly used model thanks to its reduced number of parameters (five parameters) and the appropriate trade-off between the accuracy and simplicity, particularly at low solar insulation levels. However, it requires a more entailed estimation for the values of parameters. The DDM is recognized as a model with seven parameters. Concerning the TDM, it has been reported by Khanna et al. [2] that it is a better model despite its complexity and the higher number of involved parameters (ten parameters). The reliable modeling of PV cell is a challenging task by nature, which mainly depends on the mathematical model's formulation and the accurate estimation of the key parameter values. The scenario is made even worse when the aforementioned mathematical models are implicit transcendental relationships and have this weakness to be explicitly unsolvable using the common elementary functions [16]. This intrinsic nature impedes the estimation of cell's parameters and subsequently, sizing of PV system and simulation [17]. Accordingly, it is vital to elaborate an efficient and accurate method to estimate solar cell parameters and to exceed many impediments such as lack of the variable data in the manufacturer's datasheet. In other words, the building of a reliable and accurate model based on minimal data provided in the data-sheets most often becomes mandatory and delicate. In this context and over the time, the authentic parameter identification techniques have been developed, to be transformed into an optimization problem. Inspired by this significant idea, various optimization algorithms have been deployed to process many multi-modal parameter optimization problems, especially PV cell parameters.

Parameters may be generally estimated by analytical approaches [8], numerical approaches [6], or metaheuristic approaches [2]. Although it is not as accurate as a numerical approach due to the its sophisticated simplifications that do not reflect real operational conditions, an analytical approach relies on deriving necessary mathematical equations to provide simple and fast parameter identification [18]. Furthermore, analytical approaches benefit from simplicity and fast speed for the parameter calculation. Among analytical approaches, the Lambert W-function- based method was applied for estimating the parameters of solar cell SDM [19] and DDM [20]. Lun et al. [21] developed a Taylors series expansion-based approach for SDM model of solar cells. Moreover, various varieties of analytical methods have been published in [8,22]. However, it has been approved that the accuracy of these approaches is less than that of the numerical approaches characterized by various simplifications and assumptions leading to a divergence from real operational conditions [17]. For instance, Hejri et al. [23] employed a Newton-Raphson algorithm-based numerical method using a set of approximate analytical solutions for the extraction of the five-parameter DDM model. Only the coordinates of three key points of the I-V curves have been required, which are the short and open circuit points, and the maximum power point. Since there is no analysis of the entire I-V curve and no requirement to determine two diodes ideality factors, the results contradicted the fundamental concepts. In another example [24], Laudani et al. exploited the adoption of reduced forms for the original five-parameter model. By reducing the dimensions of the search space, the convergence, the computational costs, and the execution time are severely improved. Bai et al. [7] calculated the five parameters at STC conditions using an explicit extraction method and based on five individual algebraic equations. After that, a piecewise I-V curve-fitting approach combined with the four-parameter model were exploited to adjust the five parameters under any operating condition. Mares et al. [25] developed a simple and accurate technique to estimate the five-parameter model. The limitation for the lack of the input basic manufacture data is removed. Apart from these works, other numerical approaches methods have been proposed in [6,26], but despite the improvement in accuracy, the increased number of parameters complicates the computation.

The critical study of these most conclusive works reveals the drawbacks of analytical, numerical and hybrid approaches. The analytical approaches are commonly based on approximations of converting equations into an explicit form and developed through elementary functions at particular points of the I-V and P-V characteristics. Otherwise, the simplicity and speed of calculation do not conceal the need to solve a multivariate nonlinear system, which necessarily depends on initial solutions and presents several local optima and even infinite solutions [17]. In regards to numerical approaches, they are iterative-based algorithms to treat the problem as an optimization problem and develop an objective function minimizing the error between simulated and experimental I-V and P-V characteristics [24]. Despite being more effective than the use of experimental data, numerical approaches depend on initial solutions and can frequently converge to local minima. In addition, they require higher computational resources [26]. To alleviate these drawbacks, hybrid methods are popular in the literature, yet they are not able to resolve such problems completely. However, the extreme need for the adjustment of various parameters by either a trial and error method or experiments, degrade their accuracy and increase their cost of calculation [17]. In order to mitigate the aforementioned disadvantages, metaheuristic optimizers have been proposed. Metaheuristic algorithms allowed further enhancements in this field [21]. Metaheuristic algorithms are generally iterative stochastic algorithms used to solve difficult optimization problems in various fields of operational research, engineering, or artificial intelligence [27]. Metaheuristic methods are ranging from simple local search to complex global search algorithms [28]. As stochastic techniques, metaheuristics progress towards a global optimum by sampling an objective function [29]. They behave like search algorithms, trying to learn the characteristics of a problem in order to find an approximation of the best solution. These methods, however, use a high level of abstraction, allowing them to be adapted to a wide range of different problems like estimation of unknown parameters of solar cell models [30].

According to literature, the emergence of metaheuristic algorithms began with the well-regarded Genetic Algorithm (GA) [31]. Then, the differential evolution (DE) [3] appeared followed by the optimization using the swarming particles with all of its earlier versions: PSO, PSO with velocity clamping (VCPSO) [2], and enhanced leader PSO (ELPSO) [32]. In addition to these most common approaches in solving the PV cell parameter estimation problem, recent decades witnessed the development of several new and hybrid algorithms. Despite the merits of PSO, this algorithm often shows a premature convergence that leads to low quality solutions, especially in the presence of multimodal problems such as the extraction of PV cell parameters. To alleviate this drawback, the ELPSO was proposed in [32] to mitigate the premature convergence problem based on a five-staged successive mutation strategy. These complexities have led to many other approaches for tackling the PV cell parameter estimation task such as hybrid GA-interior point [31], whale optimization algorithm (WOA) [33], ant lion optimizer (ALO) [34], and chaos optimization algorithm (COA) [35]. One of the latest metaheuristic optimizers is SSA proposed by Mirjalili et al. [36] to mimic the swarming patterns of salps in oceans. Since the development, the new SSA has gained attention due to its simplicity and acceptable efficiency. Zhao et al. [37] equipped SSA with least squares support vector machines (LSSVMs) to forecast the energy-related CO_2 emissions in China from 2014 to 2016. The results and analysis showed that the SSA-LSSVM model can show an excellent performance and enhance the accurateness and trustworthiness of CO_2 emissions forecasting. In 2018, Faris et al. [38] proposed an improved binary SSA for feature selection (FS) problems. Another asynchronous binary SSA with several leader was proposed in [39]. An SSA-based FS approach was also introduced by Hussien et al. [40] for predicting the chemical compound activities. Ekinci and Hekimoglu [41] utilized SSA for finding the parameters of power system stabilizer in multi-machine power systems. Mohapatra and Sahu [42] utilized SSA to tune the fractional order proportional-integral derivative controller. Asaithambi and Rajappa [43] used SSA to effectively realize the sizing of a CMOS

differential amplifier and the comparator circuit. SSA has also shown an efficient performance in dealing with several tasks such as finding the active power of an isolated renewable microgrid, determining the strictures of polarization curves in polymer exchange membrane fuel cells [44] and PID-Fuzzy control [45].

This paper is a seminal attempt to apply a SSA-based algorithm to the field of renewable energy. Therefore, an efficient salp swarm-inspired algorithm is proposed to tackle parameter extraction problem of the DDM model for PV cells/panels. In order to develop an appropriate objective function, a detailed modeling of the DDM model is presented. Furthermore, the exploration and exploitation mechanisms of SSA in tackling such a problem is explained in detail. To showcase the effectiveness of SSA, the obtained results are compared with both methods from existing literature such as WOA [33], ALO [34], GSA [46], novel SCA [47] and VCS [48] optimizers, which are not investigated before, despite their acceptable performance in dealing with other practical engineering cases. The performance of the proposed optimizer is tested using the values of Mean Square Error (MSE), Absolute Error (AE), and a statistical metric. The simulation results show the superior effectiveness, reliability and accuracy of the SSA-based optimizer compared to all other algorithms.

2. Mathematical modeling framework of a two-diode model based PV cell

Fig. 1 shows the different equivalent electrical circuits presented in the literature from the ideal one-diode to the generalized three-diode models.

Following Fig. 1(a), the I-V relationship is governed by:

$$I = I_{ph} - I_d = I_{ph} - I_0 \left(e^{\left(\frac{V}{\eta V_t}\right)} - 1 \right) \tag{1}$$

where I_0 (A) is the leakage current or the saturation current, I_{ph} (A) is the photo generated current, V_t is the PN junction thermal voltage related to standard test conditions (STC). V_t depends essentially on the cell temperature T (°C), the electron charge q (C), the Boltzmann constant k (J/K) and the diode ideality factor A.

The current-voltage relations of two simplified one-diode models (Fig. 1(b) and (c)) are respectively as:

$$I = I_{ph} - I_d - I_{sh} = I_{ph} - I_0 \left(e^{\left(\frac{qV}{\eta kT}\right)} - 1 \right) - \frac{V}{R_{sh}} \tag{2}$$

$$I = I_{ph} - I_d = I_{ph} - I_0 \left(e^{\left(\frac{q(V+R_sI)}{\eta kT}\right)} - 1 \right) \tag{3}$$

By taking into account the junction thermal voltage, the equivalent circuit shown in Fig. 1(d) allows to establish the non-linear function of current-voltage relationship as follows:

$$I = I_{ph} - I_d - I_{sh} = I_{ph} - I_0 \left(e^{\left(\frac{q(V+R_sI)}{\eta kT}\right)} - 1 \right) - \frac{V + R_sI}{R_{sh}} \tag{4}$$

If we suppose that the PV cells are tested under Standard Test Conditions STC (25 °C, 1000 W/m²), the previous equation shows five characteristic parameters that are: the ideality factor A, the photo-current: I_{ph} (A), the dark saturation current I_0 (A), the series resistance R_s (Ω), the shunt resistance R_{sh} (Ω). Knowing that our study subject is the double-diode model, the current-voltage relation of this photovoltaic cell model is given by:

$$I = I_{ph} - I_{d1} - I_{d2} - I_{sh} = I_{ph} - I_{01} \left(e^{\left(\frac{V+R_sI}{\eta_1 V_{t1}}\right)} - 1 \right)$$
$$- I_{02} \left(e^{\left(\frac{V+R_sI}{\eta_2 V_{t2}}\right)} - 1 \right) \frac{V + R_sI}{R_{sh}} \tag{5}$$

where I_{ph} is the photo-current generated by the incident light. I_{01} is the saturation current due to diffusion mechanism. I_{02} is the saturation current because of carrier recombination in space charge region. η_1 is the diode ideality factor for diffusion current. η_2 is the diode ideality factor for generation recombination current. V_{t1} and V_{t2} are the thermal voltages expressed by:

$$V_{t1} = V_{t2} = V_t = \frac{N_s k T}{q} \tag{6}$$

where N_s is the number of series connected PV cells in the PV panel. K is the Boltzmanns constant (1.38 10–23 J/k). The previous equation reveals the seven unknown parameters of DDM namely I_{pv}, I_{01}, I_{02}, R_s, R_{sh}, a_1, and a_2.

The knowledge of these seven parameters depends on the resolution of seven nonlinear equations that are derived from the datasheet of the PV module at STC conditions. As mentioned previously, several approaches have been used for estimating PV model parameters. Initially, analytical, numerical and hybrid approaches were proposed based on the exploitation of a series of interdependent mathematical equations to estimate different model parameters referring to the manufacturer data
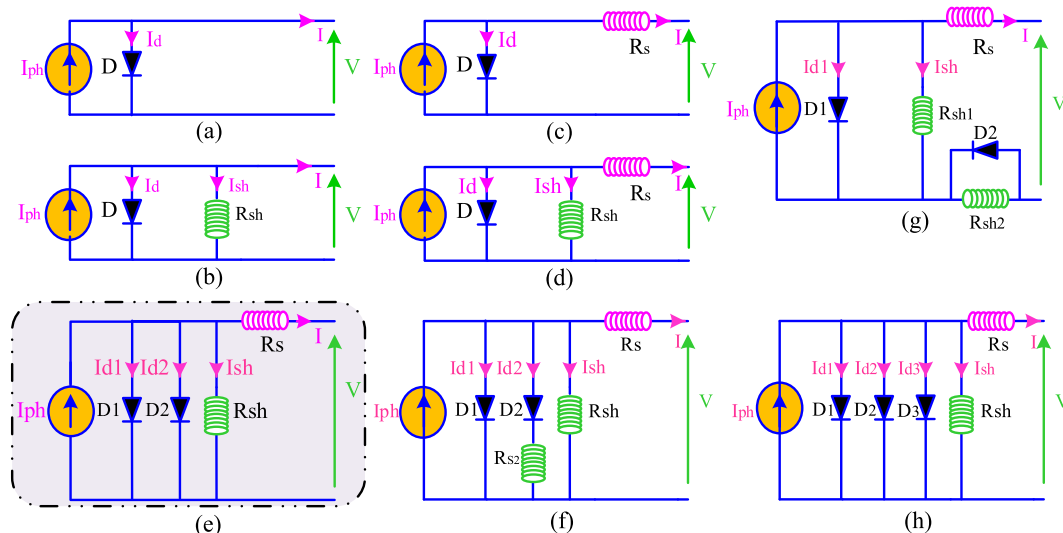

Fig. 1. Equivalent circuit of (a) the ideal one-diode PV cell model, (b) and (c) simplified one-diode models (d) practical one-diode model (e) double-diode model (f) improved double-diode model (g) reverse double-diode model (h) generalized three-diode model.

and the following particular three points (1) open-circuit voltage (OC), (2) short-circuit current (SC), and (3) maximum power point voltage and current (MPP). The strenuous assignment of solving the equations consumes monumental time and effort, mathematically. Knowing that the manufacturer provides the data at STC (1000 W/m², 25 °C), one is requested to find the seven unknown parameters at any solar irradiance and temperature. In what follows, the asterisk ($*$) denotes values measured at STC. The main rule in Eq. (5) is rewritten referring the three characteristics conditions OC, SC, and MPP by Eqs. (7)–(9), respectively.

$$0 = I_{ph}^* - I_{01}^* \left[e^{\left(\frac{V_{0c}^*}{\eta_1 V_{t1}} \right)} - 1 \right] - I_{02}^* \left[e^{\left(\frac{V_{0c}^*}{\eta_2 V_{t2}} \right)} - 1 \right] - \frac{V_{0c}^*}{R_{sh}^*} \tag{7}$$

$$I_{sc}^* = I_{ph}^* - I_{01}^* \left[e^{\left(\frac{R_{sh}^* I_{sc}^*}{\eta_1 V_{t1}} \right)} - 1 \right] - I_{02}^* \left[e^{\left(\frac{R_{sh}^* I_{sc}^*}{\eta_2 V_{t2}} \right)} - 1 \right] - \frac{R_s^* I_{sc}^*}{R_{sh}^*} \tag{8}$$

$$I_{mpp}^* \left(1 + \frac{R_s^*}{R_{sh}^*} \right) = I_{01}^* \left[e^{\left(\frac{V_{0c}^*}{\eta_1 V_{t1}} \right)} - \frac{V_{mpp}^* + R_s^* I_{mpp}^*}{\eta_1 V_{t1}} \right]$$
$$+ I_{02}^* \left[e^{\left(\frac{V_{0c}^*}{\eta_2 V_{t2}} \right)} - \frac{V_{mpp}^* + R_s^* I_{mpp}^*}{\eta_2 V_{t2}} \right] + \frac{V_{0c}^* - V_{mpp}^*}{R_{sh}^*} \tag{9}$$

With respect to V, the power supplied by the PV module is differentiated as:

$$\frac{dP}{dV} = \frac{d(I \cdot V)}{dV} = \frac{dI}{dV} \cdot V + I \tag{10}$$

By differentiating the rule in Eq. (5) with respect to voltage one can obtain the quantity $\frac{dI}{dV}$:

$$\frac{dI}{dV} = -\frac{I_{01}}{\eta_1 V_{t1}} \left(1 + R_s \frac{dI}{dV} \right) exp \left(\frac{V + R_s I}{\eta_1 V_{t1}} \right)$$
$$- \frac{I_{02}}{\eta_2 V_{t2}} \left(1 + R_s \frac{dI}{dV} \right) exp \left(\frac{V + R_s I}{\eta_1 V_{t1}} \right) - \frac{1}{R_{sh}} \left(1 + R_s \frac{dI}{dV} \right) \tag{11}$$

At the MPP, the term $\frac{dP}{dV}$ is zero. This leads to:

$$\frac{dI}{dV} = -\frac{I_{mpp}^*}{V_{mpp}^*} \tag{12}$$

It can be obtained that:

$$\frac{I_{mpp}^*}{I_{mpp}^*} = \frac{I_{01}}{\eta_1 V_{t1}} \left(1 - R_s^* \frac{I_{mpp}^*}{I_{mpp}^*} \right) exp \left(\frac{V_{mpp}^* + R_s^* I_{mpp}^*}{\eta_1 V_{t1}} \right)$$
$$+ \frac{I_{02}}{\eta_2 V_{t2}} \left(1 - R_s^* \frac{I_{mpp}^*}{I_{mpp}^*} \right) exp \left(\frac{V_{mpp}^* + R_s^* I_{mpp}^*}{\eta_1 V_{t1}} \right) - \frac{1}{R_{sh}^*} \left(1 - R_s^* \frac{I_{mpp}^*}{I_{mpp}^*} \right) \tag{13}$$

The extraction of I_{ph} using Eq. (7) and its substitution in Eqs. (8) and (9), result in Eqs. (14) and (15), respectively:

$$I_{sc}^* = I_{01}^* \left[exp \left(\frac{I_{sc}^*}{\eta_1 V_{t1}} \right) - exp \left(\frac{R_s^* I_{sc}^*}{\eta_1 V_{t1}} \right) \right] - I_{02}^* \left[exp \left(\frac{V_{0c}^*}{\eta_2 V_{t2}} \right) - exp \left(\frac{R_s^* I_{sc}^*}{\eta_2 V_{t2}} \right) \right]$$
$$+ \frac{V_{0c}^* - R_s^* I_{sc}^*}{R_{sh}^*} \tag{14}$$

$$I_{mpp}^* \left(1 + \frac{R_s^*}{R_{sh}^*} \right) = I_{01}^* \left[exp \left(\frac{V_{0c}^*}{\eta_1 V_{t1}} \right) - exp \left(\frac{V_{mpp}^* + R_s^* I_{mpp}^*}{\eta_1 V_{t1}} \right) \right]$$
$$+ I_{02}^* \left[exp \left(\frac{V_{0c}^*}{\eta_2 V_{t2}} \right) - exp \left(\frac{V_{mpp}^* + R_s^* I_{mpp}^*}{\eta_2 V_{t2}} \right) \right]$$
$$+ \frac{V_{0c}^* - V_{mpp}^* *}{R_{sh}^*} \tag{15}$$

The three independent equations Eqs. (13)–(15) show four unknown variables I_{01}, I_{02}, R_s, and R_{sh}. The derivative of the current with respect to the voltage at the open circuit voltage ($I = 0$ and $V = V_{0c}$) and at the short circuit current ($I = I_{sc}$ and $V = 0$) gives Eqs. (16) and (17), respectively:

$$\frac{dI}{dV} = -\frac{1}{R_s} \tag{16}$$

$$\frac{dI}{dV} = -\frac{1}{R_{sh}} \tag{17}$$

Starting from a zero initial value of R_s ($R_{s0} = 0$), the initial value of R_{sh} is expressed by Eq. (18):

$$R_{sh0} = \frac{V_{mpp}}{I_{sc}^* - V_{mpp}} - \frac{V_{0c}^* - V_{mpp}}{I_{mpp}} \tag{18}$$

At this stage, R_s and R_{sh} can be calculated simultaneously by iteratively increasing the value of R_s while calculating R_{sh}. At the characteristic MPP point, the resistance R_{sh} becomes:

$$R_{sh}$$
$$= \frac{V_{mpp} + R_s I_{mpp}}{I_{ph} - I_{01} \left[exp \left(\frac{V_{mpp} + R_s I_{mpp}}{\eta_1 V_{t1}} \right) + exp \left(\frac{V_{mpp} + R_s I_{mpp}}{\eta_2 V_{t2}} \right) + 2 \right] - \frac{P_{mpp,E}^* - R_s^* I_{sc}^*}{V_{mpp}}} \tag{19}$$

Here, $P_{mpp,E}^*$ is the maximum power of manufacturers datasheet.

Following the determination of the key parameters by numerical methods under the STC conditions, the exportation of such parameters to real outdoor conditions is required using following equations. Under a determined solar radiation and a temperature, the photo-current I_{ph} is:

$$I_{ph} = (I_{ph}^* + K_i(T - T^*)) \frac{G}{G^*} = \left(I_{sc}^* \frac{R_{sh} + R_s}{R_{sh}} + K_i(T - T^*) \right) \frac{G}{G^*} \tag{20}$$

where, K_i is temperature coefficient of SC current ($A/°C$).

The reverse saturation currents are written as follows:

$$I_0 = I_{01} = I_{02} = \frac{I_{sc}^* + K_i(T - T^*)}{exp \left(\frac{V_{0c}^* + K_v(T - T^*)}{\eta_1 V_t} \right) - 1} \tag{21}$$

where, K_v is temperature coefficient of OC voltage ($V/°C$).

At this stage, one can establish the following parameters under any weather condition:

$$I_0 = I_{01} = I_{02} = \frac{I_{sc}^* + K_i(T - T^*)}{exp \left(\frac{V_{0c}^* + K_v(T - T^*) + \eta V_t ln \left(\frac{G}{G^*} \right)}{\eta_1 V_t} \right) - 1} \tag{22}$$

$$I_{sc}(G, T) = I_{sc}^* \frac{G}{G^*} + K_i(T - T^*) \tag{23}$$

$$V_{0c}(G, T) = V_{0c}^* - K_v(T - T^*) \frac{G}{G^*} + \eta V_t ln \left(\frac{G}{G^*} \right) \tag{24}$$

$$I_{mpp}(G, T) = I_{mpp}^* \frac{G}{G^*} \tag{25}$$

$$V_{mpp}(G, T) = V_{mpp}^* \frac{G}{G^*} - K_v(T - T^*) \tag{26}$$

Though the DDM model has gained attention owing to its superior accuracy compared to SDM, the evaluation of its seven key parameters remains more difficult. Therefore, numerous methods namely analytical, numerical hybrid, and metaheuristic ones were carried out to resolve this problem. Knowing that the execution time is an important factor and since the requirements of analytical approaches are limited to analyze only key points of I-V curve, the number of iteration is much reduced. Despite this merit, the accuracy is decreased. Concerning the

numerical extractions, they imply also several drawbacks in terms of high situational and execution speed.

With recent soft computing popularity, the hybrid methods were proposed without being able to overcome the aforementioned disadvantages, which are incorporating analytical methods to relate parameters variations with temperature, irradiation, and EA numerical methods for optimization. With regards to these shortcomings, the following section reveals an efficient and accurate SSA-based algorithm for the two-diode model.

3. SSA-based proposed method

SSA is a novel meta-heuristic optimizer recently proposed by Mirjalili et al. [36] to efficiently tackle optimization problems. Salp is classified under a class of Salpidae family. The swarming nature of salps is very noticeable because they can construct collaborative chains during foraging activities in deep oceans. This behavior assists salps in gaining more kinetic energy throughout pursuing of the food source. The idea of SSA algorithm is inspired by the swarming tactics of salps through generating the salp chain. The salp chains can assist SSA in mitigating the inertia to the local optima (LO) to some extent. However, SSA cannot always carry out a suitable balance between the exploration and exploitation processes. Therefore, the original method occasionally fails to attain a high quality global optimum in some real-world cases.

In SSA, salp chain consists of two classes of salps, which are leader and followers. The leader is a salp located at the head of the chain, whereas other members play the role of followers. Leader salp guides the direction and locomotion of swarm, while the followers make use of other peers. A conceptual design of salp chain is demonstrated in Fig. 2.

In SSA, the position vector of each salp is defined for searching in an n-dimensional space, where n is number of decision variables. The population of SSA X will consist of N salps with d-dimensions. Therefore, population vector is made by a $N \times d$-dimensional matrix, as shown in Eq. (27):

$$X_i = \begin{bmatrix} x_1^1 & x_2^1 & \dots & x_d^1 \\ x_1^2 & x_2^2 & \dots & x_d^2 \\ \vdots & \vdots & \dots & \vdots \\ x_1^N & x_2^N & \dots & x_d^N \end{bmatrix} \tag{27}$$

In SSA, the food source is the target location of all salps. Hence, the position of leader is obtained by Eq. (28):

$$x_j^1 = \begin{cases} F_j + c_1((ub_j - lb_j)c_2 + lb_j) & c_3 \geqslant 0.5 \\ F_j - c_1((ub_j - lb_j)c_2 + lb_j) & c_3 < 0.5 \end{cases} \tag{28}$$

where x_j^1 is the leaderś position and F_j is the position of food source in the

jth dimension, ub_j is the upper limit of jth dimension, and lb_j is the lower limit of jth dimension, c_2 and c_3 are random vectors generating values inside [0, 1], and c_1 is the core parameter of SSA formulated as in Eq. (29):

$$c_1 = 2e^{-\left(\frac{4t}{T_{max}}\right)^2} \tag{29}$$

where t shows the current iteration, and T_{max} shows the maximum number of iterations. The former parameter c_1 can make the exploration and exploitation tendencies of SSA in a balanced state. The position of follower salps are revised by Eq. (30):

$$x_j^i = \frac{x_j^i + x_j^{i-1}}{2} \tag{30}$$

where $i \geqslant 2$ and x_j^i denotes the state of ith salp at the jth dimension.

To apply the SSA-based approach, Eq. (5) can be re-expressed as:

$$f(V_t, I_t, r) = I_t - I_{ph} - I_{01}\left(e^{\left(\frac{V_t + R_s I}{\eta_1 V_{t1}}\right)} - 1\right) - I_{02}\left(e^{\left(\frac{V_t + R_s I}{\eta_2 V_{t2}}\right)} - 1\right)\frac{V_t + R_s I}{R_{sh}} \tag{31}$$

where $r = [I_{ph} R_s R_{sh} I_{01} I_{02} a_1 a_2]$ are the parameters to be estimated. After each iteration, the values in r is updated and then checked if it has converge to the correct value. The procedure ends when intended maximum number of iteration has been reached. To objectively evaluate the performance of the SSA method, an objective function F is introduced. The objective function established in this work is given by:

$$F = \sqrt{\frac{1}{N}\sum_1^N (f(V_t, I_t, r))^2} \tag{32}$$

subject to

$$I_{phmin} \leqslant I_{ph} \leqslant I_{phmax} \tag{33}$$

$$R_{smin} \leqslant R_s \leqslant R_{smax} \tag{34}$$

$$R_{shmin} \leqslant R_{sh} \leqslant R_{shmax} \tag{35}$$

$$I_{01min} \leqslant I_{01} \leqslant I_{01max} \tag{36}$$

$$I_{02min} \leqslant I_{02} \leqslant I_{02max} \tag{37}$$

$$a_{1min} \leqslant a_1 \leqslant a_{1max} \tag{38}$$

$$a_{2min} \leqslant a_2 \leqslant a_{2max} \tag{39}$$

where I_t and V_t are the experimental data describing the current-voltage curves, and N is the number of data. Hence, the optimization algorithm is based on the minimization of the fitness function with respect to the parameters bounds. A smaller value of F implies a least deviation between the data and the one simulated by the SSA-proposed approach. The pseudo-code of the proposed SSA-based algorithm is shown in Algorithm 1.

Algorithm 1. Pseudo-code of SSA-based approach

Initialize the random initial population of salps $x_i (i = 1, 2, ..., n)$
while (stopping condition is not valid) **do**
    Calculate the fitness of all salps using Eq. (31)
    Find the best salp and set it as **F**, the leader salp
    Update c_1 by Eq. (29)
    for (every salp (x_i)) **do**
        if ($i == 1$) **then**
            Update the state of leader by Eq. (28)
        else
            Update the state of followers by Eq. (30)
    Update all salps based on the superior and inferior limits of variables
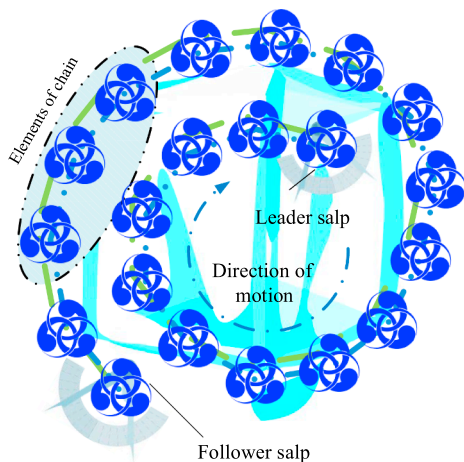   Brought back the search agents that violated the constraints in Eqs. (33)–(39).
Return **F**

Fig. 2. Illustration of a salp chain.

Elements of chain

Leader salp

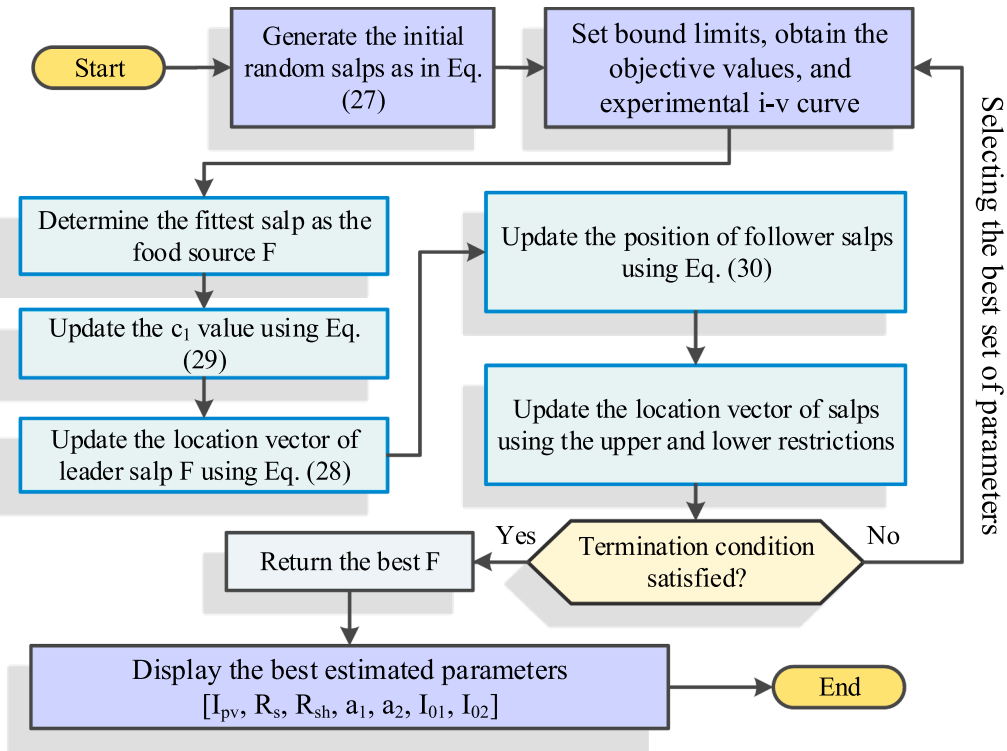Direction of motion

Follower salp

Fig. 3. Flowchart of the proposed SSA-based parameter extraction technique.

Referring to Algorithm 1, the SSA-based method randomly distributes all search agents (salps) over the solution space. Then, it assesses the current population of salps to detect the leading salp. All salps try to follow the front-runner salp (leader) as shown in Fig. 2. In this process, the variable c_1 is updated by Eq. (29). The rule in Eq. (28) helps SSA to inform the state of leader, while Eq. (30) changes the position of the other salps. Until satisfying the stopping condition, all steps excluding the initialization phase will be repeated to upsurge the quality of salps as much as possible. The flowchart of the SSA-based approach is also shown in Fig. 3.

4. Experimental results and analysis

In this section, the results of different methods including SSA are compared in terms of convergence rate and quality of results. To investigate the efficacy of SSA in solving this problem, it is compared to several state-of-the-art methods such as Gravitational Search Algorithm (GSA) [46], Sine Cosine Algorithm (SCA) [47], Whale Optimization Algorithm (WOA) [49], Ant Lion Optimizer (ALO) [50], and Virus Colony Search (VCS) [48]. These recent, well-established approaches have shown several advantages in terms of performance and quality of solutions in previous researches. Therefore, they can be considered as the state-of-the-art comparative methods to see how competitive the proposed SSA-based method is. Note that the controlling parameters of all algorithms are set based on the recommendations in the original papers [36,46–50]. All results are obtained based on the overall outcomes of 30 randomly-initialized independent runs and during 100 internal iterations to evolve 30 search agents in each algorithm. All results obtained in this research are recorded using a single computer, and all tests are carried out in a same condition to have a fair comparison. For testing and programming, MATLAB 2015 software is used to perform all tests. Details of the hardware and software is presented in Table 1.

In this paper, two different cases are considered for evaluating the

**Table 1**
The detailed settings of the utilized system.

Name	Setting
Hardware	
CPU	Intel Core(TM) i3-5200U
Frequency	2.2 GHz
RAM	4 GB
Hard drive	500 GB
Software	
Operating system	Windows 7
Language	MATLAB R2015a

performance of algorithms based on the extracted parameters. The experimental datasets utilized in these cases are acquired from [16].
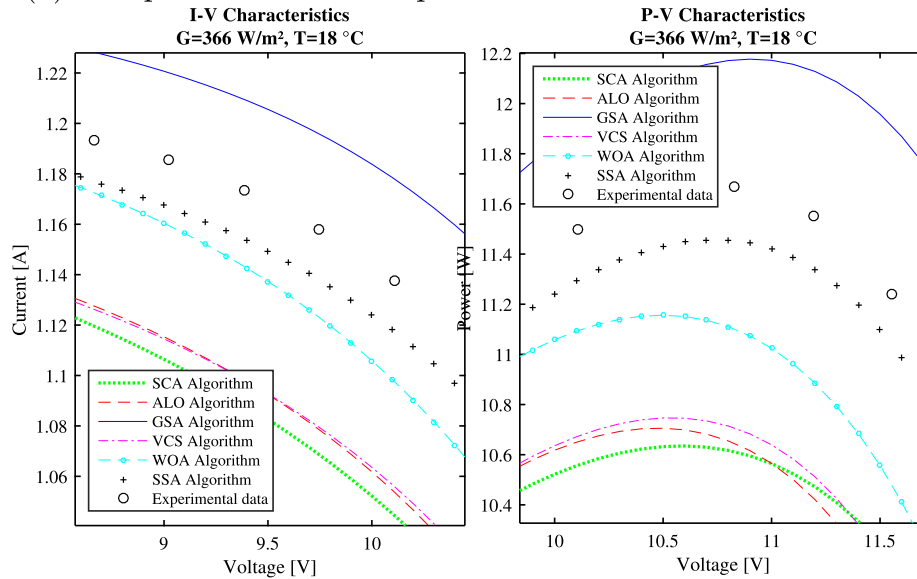
4.1. I-V and P-V characteristics

In this subsection, the illustrated characteristics of two different experimental cases and the extracted parameters by various algorithms including SSA, GSA, ALO, VCS, SCA, and WOA are compared based on different metrics. Fig. 4 shows the comparative results including the curve's characteristics performed by six algorithms at $G = 366$ W/m^2 and $T = 18$ °C. It can be observed from Fig. 4 that the proposed SSA-based algorithm shows a superior agreement between the generated characteristics and experimental data. For these low climate conditions, it is observed that all algorithms perform similarly around the short circuit and the open voltage points with a neglected error. Therefore, the significant choice between these algorithms can be often attained in the maximum power point (MMP). In this point, the proposed SSA-based algorithm can also be considered as the best technique compared to other peers. Based on results, the WOA obtains the second best value around this MPP point, which is followed by the GSA, ALO, VCS, and SCA algorithms.

The main reason for the improvements in the results of SSA is that the proposed method can establish a fine and more consistent balance
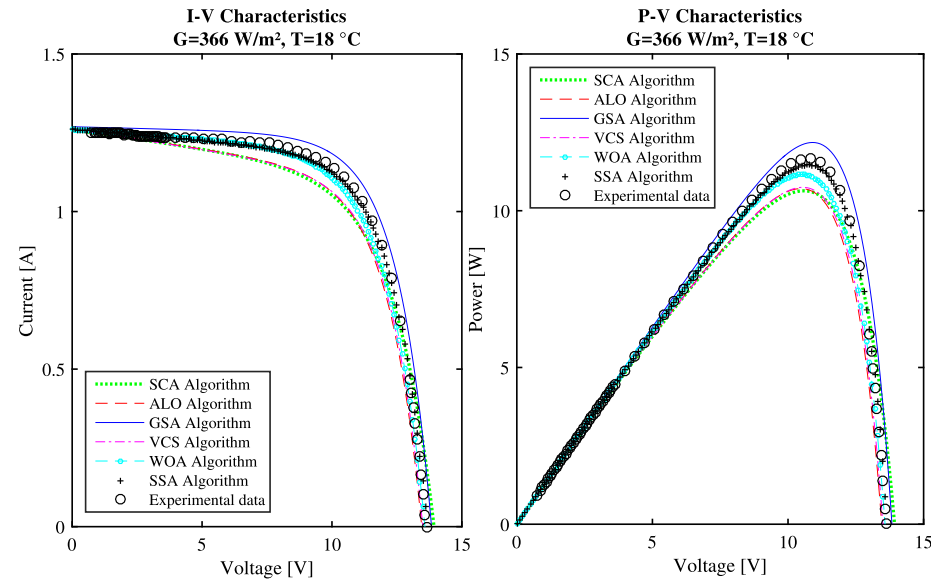
(a) Comparison between experimental data and simulated results
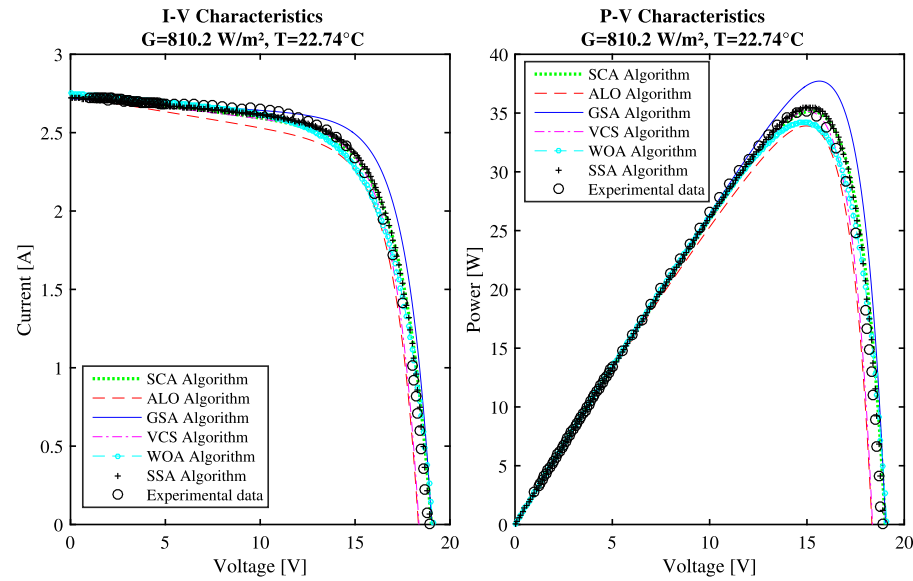

(b) A closer window

Fig. 4. Comparison between experimental data and simulated results for each algorithm: Current-Voltage and Power-Voltage characteristics at $G = 366$ W/m^2, $T = 18$ °C.

between the exploration and exploitation trends. The SSA also shows more flexibility, higher exploratory and exploitative behaviors as compared to other methods. It starts the process by broad exploration and continue with more exploitation trends in last steps. This behavior assists SSA in exploring more high quality solutions compared to other method in dealing with parameters identification of DDM PV cell problem. In the case of LO stagnation, efficient time-varying mechanisms of SSA help to jump out and scan vicinity of other explored solutions. However, the observed curves for I-V and P-V Characteristics reveal that SCA, VCS, GSA, and ALO approaches failed to make a stable balance between exploration and exploitation, and local optima stagnation is evident. As a result, the error of simulated results has increased.

In this work, the climatic conditions with high temperature and irradiation are also considered as second experimental case. Fig. 5 compares the resulted curves for characteristics simulated by all algorithms at $G = 810.2$ W/m^2 and $T = 22.74$ °C. As previously observed for the first real case, the curve obtained by SSA again shows the minimum

errors and there is a high agreement between the experimental and simulated data in dealing with the second case. It can be observed that all compared algorithms obtain the same results in the short circuit point. Nevertheless, the I-V and P-V characteristics presented in Fig. 5 also show that some differences can be detected between the experimental and simulated data obtained based on other used algorithms. In the maximum power and open voltage points, GSA, VCS and ALO algorithms demonstrate less satisfactory performance compared to other algorithms. The results for second case confirm the improved performance of the SSA-based method in terms of exploration and exploitation tendencies and LO avoidance capacities, while this observation is not seen in the results of other algorithms such as SCA, GSA, and ALO.

The main observation is that the exploration power of the ALO algorithm is mainly dependent on the random selection of ant lions and the random walk process of agents around the best solutions. Then, it focuses on the promising regions around the high quality solutions based on an adaptive shrinking mechanism to construct the ant lions

(a) Comparison between experimental data and simulated results
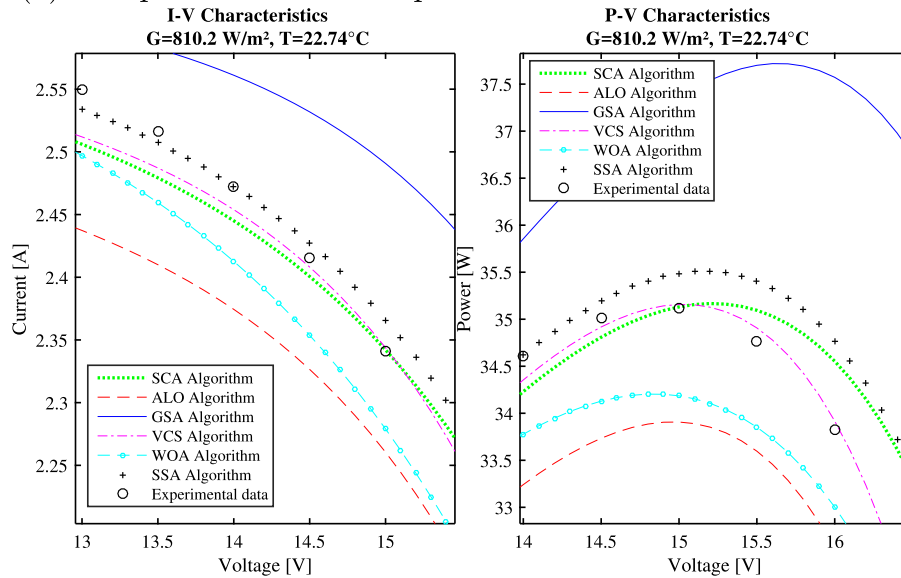
(b) A closer window

Fig. 5. Comparison between experimental data and simulated results for each algorithm: Current-Voltage and Power-Voltage characteristics at $G = 810.2$ W/m², $T = 22.74$ °C.

traps. However, ALO is not always stable enough to make a smooth transition from exploration to exploitation. Despite the observed unbalanced behaviors of ALO, the exploratory and exploitative mechanisms of SSA show better stability. Hence, there is a lower difference between the simulated results and experimental data, and it finds more high-quality solutions after a certain number of iterations. In the case of VCS, the virus's diffusion phase is performed based on the Gaussian random walk approach. It also utilizes the weighted mean of the best agents, which in general, we observed that these strategies has increased the inertia of VCS to be stagnated to LO when dealing with landscape of this problem. In addition, the ALO and VCS have more fixed controlling parameters that considerably change the exploratory and exploitative behaviors of the optimizer, while the SSA and SCA have fewer static parameters and they are equipped with more efficient time-varying mechanisms for making a more stable balance between exploration and exploitation trends. This difference has also led to obtain fitter results when using the proposed SSA-based approach,

while the SCA also has shown a competitive efficacy.

When comparing the results of GSA with SSA, we see the simulated curve of GSA are not in accordance with the experimental data, while the curves of SSA are more satisfying. The reason is that the solutions with heavy inertia mass in GSA will update their position vectors more slowly. As such, they will explore the solution space more locally. Additionally, we observed that the gravitational constant could not consistently adjust the accuracy of the exploration and exploitation. Hence, it fails to make a good trade-off between the global and local phases and it gets trapped in LO. This behavior is not observed in the proposed SSA-based method due to the role of c_1 parameter. Hence, we see the simulated results of SSA are better than GSA.

Inspecting the simulated curve of WOA, it is evident that the discrepancy is higher than SSA. The reason that WOA does not outperform SSA in this case is that WOA starts the search with high exploration (searching for the prey) and using the random leaders, it tries to explore various regions of the feature space. In the exploitation phase, however,

Table 2
Extracted parameters of two considered cases.

Parameters	I_{pv}	R_s	R_{sh}	a_1	a_2	I_{01}	I_{02}
			$G = 366$ W/m², $T = 18$ °C				
SCA	1.259	0.168	87	1.556	1.2	1.1e−4	1.1e−4
ALO	1.260	0.489	82	1.02	1.02	1.697e−05	1.868e−05
GSA	1.269	0.348	485.997	1.030	1.005	1.499e−05	1.440e−05
VCS	1.261	0.463	78.708	1	1	1.399e−05	1.399e−05
WOA	1.260	0.451	180	1.1	1.52	7e−05	7e−05
SSA	1.260	0.341	145	1.02	1.001	1.45e−05	1.45e−05
			$G = 810.2$ W/m², $T = 22.74$ °C				
SCA	2.74	0.169	72.000	1.456	1.200	9e−6	9e−6
ALO	2.733	0.489	50	1	1	6.869e−07	6.786e−07
GSA	2.716	0.818	140.659	1.013	1.058	6.999e−07	6.405e−07
VCS	2.734	0.333	70.189	1.003	1.002	6.990e−07	6.993e−07
WOA	2.75	0.351	90	1.60	1.48	7e−05	7e−05
SSA	2.722	0.174	98	1.2	1.3	7.8e−06	7.8e−06

it intensifies a shrinking encircling process. We observed that the WOA algorithm has an inertia to LO due to the role of *A* parameter.

Table 2 shows the extracted parameters of the DDM for the solar panel. To investigate the accuracy of the proposed SSA-based method compared to other algorithms, the well-known Mean Square Error (*MSE*) and the Absolute Error (*AE*) are employed in this research. These metrics can be defined as in Eqs. (40) and (41) [17]:

$$MSE = \sqrt{\frac{\sum_{i=1}^{N}(I_{measured} - I_{simulated})^2}{N}} \qquad (40)$$

$$AE(\%) = 100|I_{measured} - I_{simulated}| \qquad (41)$$

Table 3 shows the results in terms of *AE* for different approaches. From Table 3, all *AE* values are almost around 5% except those obtained by the SCA, ALO, VCS algorithms in the maximum power point, where can reach to the area of 10%. In the first case, the SSA algorithm provides a superior performance and attains the highest accuracy rates by finding the best *AE* values in different operating points. Based on *MSE* results, the values of all presented algorithms are below 1.9115e−03, which confirm and validate the accuracy of the identified parameters. The *MSE* results also show that the SSA-based method outperforms other peers in exploration and exploitation of the target space. Hence, it can avoid LO more effectively and detect more high-quality parameters with higher accuracy rates.

Table 2 shows the extracted parameters used to generate the curves characteristics of the DDM of solar panel at $G = 810.2$ W/m² and $T = 22.74$ °C. In this case, the *MSE* value of the proposed SSA is the ranked one compared to all other algorithms by 1.5777e−06 and its *AE* values for different characteristic points do not exceed 2% as shown in Table 3.

The MSE results are also compared visually in Fig. 6. As per visualizations, the SSA covers a small portion of the whole area when $G = 366$ W/m², $T = 18$ °C (see Fig. 6b), while in Fig. 6a (when $G = 366$ W/m², $T = 18$ °C), it shares 1.181% of the whole area.

4.2. Statistical analysis and objective function evaluation

The convergence curves of different algorithms are presented in Fig. 7. From Fig. 7, it can be observed that the average fitness function of all algorithms varies in an acceptable margin. In addition, SSA shows the fastest convergence rate. It is observed that VCS shows some stagnation behaviors, and there is a delay in converging to the minimum function values. The GSA algorithm also has converged to the LO and it has not escaped from it, effectively. Based on convergence inclinations, the SCA, ALO and WOA algorithms are in the next places. The reason for the fast convergence speed of the proposed SSA-based technique is that it starts the searching process with a more extensive exploration, and then it focuses more on the local search. Hence, it shows a better convergence behavior and more potential in escaping from the LO and hence, finding more high-quality solutions.

As per results in Table 4, it can be observed that the proposed SSA-based method outperforms other peers and finds the best results (0.31487) in terms of average results. The SD_F results also indicate the SSA can show higher stability in dealing with these real-world cases. In terms of reliability of the extracted parameters, it is obvious that the proposed SSA algorithm outperforms other five algorithms by 0.00028 of standard deviation. The second best results in terms of accuracy and reliability are attained by SCA and WOA algorithms, respectively. Based on SD_F results, SSA is ranked one followed by SCA, WOA, VCS, ALO, and GSA, respectively. According to best results, top three methods are SSA, WOA, and VCS. The best results reveal all methods in terms of best results are very competitive, but the proposed SSA-based approach can find slightly better solutions. From these results, it can be stated that the SSA-based parameter extraction method can provide results that are more preferable than other presented algorithms in both low and high climate conditions. The SSA benefits from more efficient time-varying mechanisms. Therefore, not only it has more potential to make a stable balance between the exploration and exploitation trends but also it can switch between broad exploration and focused exploitation, more smoothly.

From the previous results and analysis, we can conclude that the SSA algorithm has proven its advantages including fast convergence, stable balance between exploration and exploitation and high capacity in escaping LO in stagnation conditions in dealing with parameters identification problem of photovoltaic cell/panel/module.
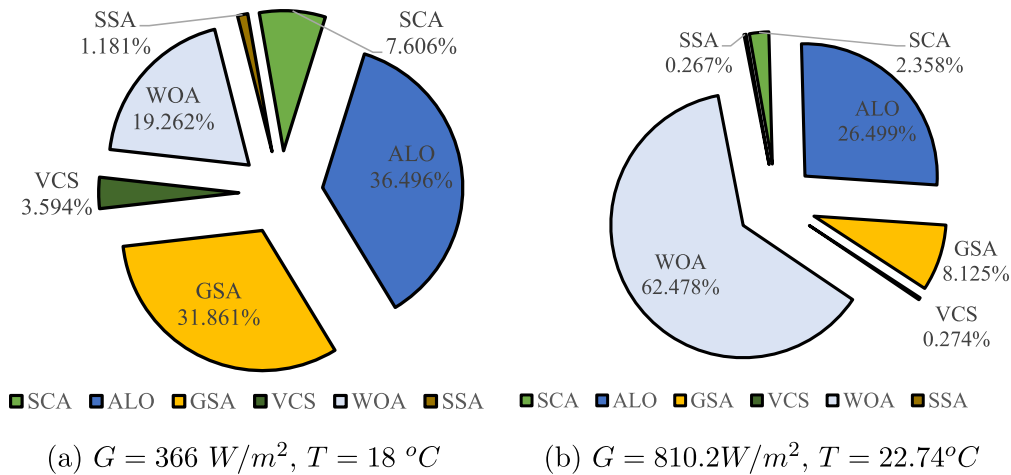
Table 3
AE and *MSE* on three remarkable points for different algorithms.

		SCA	ALO	GSA	VCS	WOA	SSA
				$G = 366$ W/m², $T = 18$°C			
AE(%)	I_{sc}	0.7	0.9	1.7	0.9	0.8	0.9
	I_m	5	4.5	3	4.6	1.8	0.8
	V_m	10	8.5	6	9	2.5	1
	V_{0c}	5	7	5.5	7	6	0.5
MSE		1.9115e−03	9.1716e−03	8.0067e−03	9.0306e−04	4.8405e−03	**2.9681e−04**
				$G = 810.2$ W/m², $T = 22.74$°C			
AE(%)	I_{sc}	2	1.3	0.4	1.4	3	0.4
	I_m	0.5	4.1	4.3	0.7	2.4	0.1
	V_m	5	6.2	8	3	4	1.87
	V_{0c}	6	7.65	4.87	7.5	3.034	2.012
MSE		1.3937e−05	1.5665e−04	4.8032e−05	1.6188e−06	3.6935e−04	**1.5777e−06**

(a) $G = 366 \ W/m^2$, $T = 18 \ ^oC$ (b) $G = 810.2 W/m^2$, $T = 22.74^oC$

Fig. 6. Visual comparison of MSE results for different algorithms and conditions.
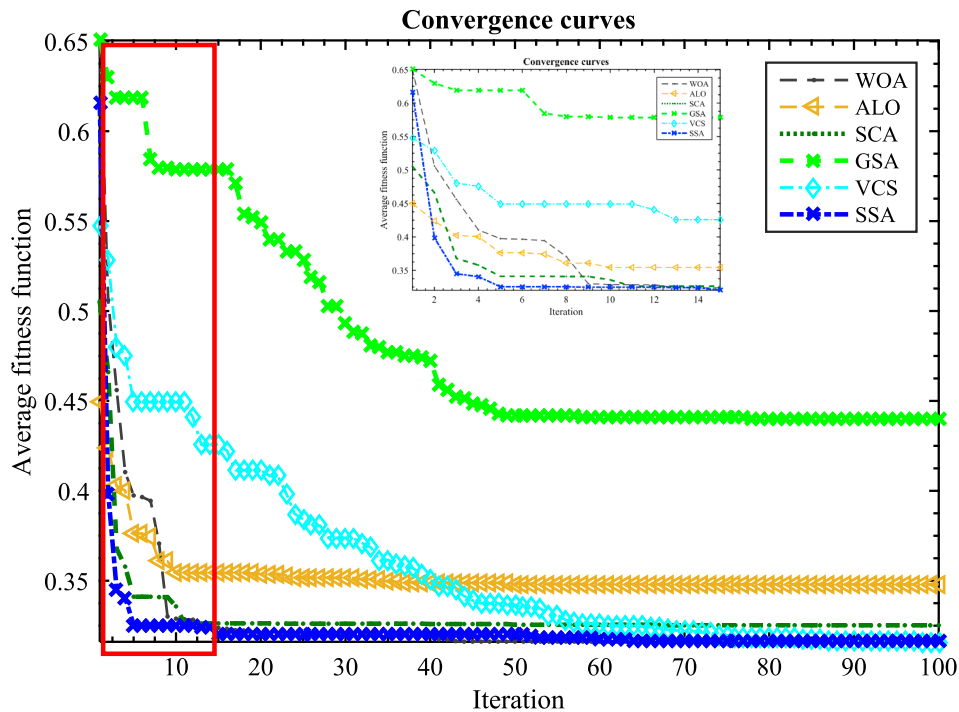

Fig. 7. Convergence curves for different algorithms.

Table 4
Statistical analysis of obtained results.

Algorithms	Min_F	Max_F	Ave_F	SD_F
SCA	0.31558	0.31621	0.31599	0.00035
ALO	0.31674	0.35126	0.33068	0.01819
GSA	0.49424	0.56884	0.54253	0.04187
VCS	0.31576	0.31693	0.31622	0.00062
WOA	0.31531	0.31618	0.31581	0.00045
SSA	**0.31487**	**0.315375**	**0.31504**	**0.00028**

5. Conclusions and future directions

This paper proposed a new SSA-based technique for seven parameters identification of DDM PV cell models. The parameters identification of DDM PV cell was modeled as an optimization task and the proposed SSA-based approach was first compared to the novel SCA and VCS optimizers that are not used before in this application. The

proposed method was then compared to well-established algorithms such as ALO, GSA, and WOA. The main conclusions of this work are summarized as follows:

- The outdoor experiments applied to TITAN-12-50 panel were conducted to validate the DDM PV model under different climatic conditions.
- The MSE and AE metrics were utilized to evaluate and compare the performance of all studied algorithms.
- A statistical criterion used for improving the choice between the different methods such as the minimum, maximum and standard deviation of the objective function, which showed the superiority of the SSA.
- SSA shows more flexibility thanks to its ability to establish a more stable balance between the exploration and exploitation inclinations.
- The good fitness and the excellent matching with the experimental I-V and P-V characteristics confirms the better reliability and stability

of the proposed SSA-based technique.

These results confirm that the proposed SSA-based algorithm is promising and can be considered as a valuable tool for PV cell parameter extraction since it achieves better performance in tackling the nonlinear equations of the investigated problem. For future works, we recommend to exploit and improve the SSA and other metaheuristic algorithms for further benefits in this field and other renewable energy and power systems.

Acknowledgement

References

[1] Peng L, Sun Y, Meng Z. An improved model and parameters extraction for photovoltaic cells using only three state points at standard test condition. J Power Sources 2014;248:621–31.

[2] Khanna V, Das BK, Bisht D, Vandana, Singh PK. A three diode model for industrial solar cells and estimation of solar cell parameters using pso algorithm. Renew Energy 2015;78:105–13.

[3] Hultmann Ayala HV, Coelho LdS, Mariani VC, Askarzadeh A. An improved free search differential evolution algorithm: a case study on parameters identification of one diode equivalent circuit of a solar cell module. Energy 2015;93:1515–22.

[4] Ma T, Yang H, Lu L. Development of a model to simulate the performance characteristics of crystalline silicon photovoltaic modules/strings/arrays. Sol Energy 2014;100:31–41.

[5] Bana S, Saini RP. Identification of unknown parameters of a single diode photovoltaic model using particle swarm optimization with binary constraints. Renew Energy 2017;101:1299–310.

[6] Ayodele TR, Ogunjuyigbe ASO, Ekoh EE. Evaluation of numerical algorithms used in extracting the parameters of a single-diode photovoltaic model. Sustain Energy Technol Assess 2016;13:51–9.

[7] Bai J, Liu S, Hao Y, Zhang Z, Jiang M, Zhang Y. Development of a new compound method to extract the five parameters of pv modules. Energy Convers Manage 2014;79:294–303.

[8] Batzelis EI, Papathanassiou SA. A method for the analytical extraction of the single-diode pv model parameters. IEEE Trans Sustain Energy 2016;7:504–12.

[9] Sudhakar Babu T, Prasanth Ram J, Sangeetha K, Laudani A, Rajasekar N. Parameter extraction of two diode solar pv model using fireworks algorithm. Sol Energy 2016;140:265–76.

[10] Suskis P, Galkin I. Enhanced photovoltaic panel model for matlab-simulink environment considering solar cell junction capacitance. IECON 2013 – 39th annual conference of the IEEE industrial electronics society. 1613. p. 1613–8.

[11] Ken-ichi K, Hiroyuki M. New two-diode model for detailed analysis of multicrystalline silicon solar cells. Jpn J Appl Phys 2005;44:8314.

[12] Mazhari B. An improved solar cell circuit model for organic solar cells. Sol Energy Mater Sol Cells 2006;90:1021–33.

[13] De Castro F, Laudani A, Riganti Fulginei F, Salvini A. An in-depth analysis of the modelling of organic solar cells using multiple-diode circuits. Sol Energy 2016;135:590–7.

[14] Lumb MP, Bailey CG, Adams JGJ, Hillier G, Tuminello F, Elarde VC, et al. Analytical drift-diffusion modeling of gaas solar cells incorporating a back mirror. IEEE 39th photovoltaic specialists conference (PVSC). 2013. p. 1063–8.

[15] Soon JJ, Low KS. Optimizing photovoltaic model for different cell technologies using a generalized multidimension diode model. IEEE Trans Industr Electron 2015;62:6371–80.

[16] Abbassi A, Gammoudi R, Ali Dami M, Hasnaoui O, Jemli M. An improved single-diode model parameters extraction at different operating conditions with a view to modeling a photovoltaic generator: a comparative study. Sol Energy 2017;155:478–89.

[17] Abbassi R, Abbassi A, Jemli M, Chebbi S. Identification of unknown parameters of solar cell models: a comprehensive overview of available approaches. Renew Sustain Energy Rev 2018;90:453–74.

[18] Muhsen DH, Ghazali AB, Khatib T, Abed IA. A comparative study of evolutionary algorithms and adapting control parameters for estimating the parameters of a single-diode photovoltaic module's model. Renew Energy 2016;96:377–89.

[19] Dhass AD, Lakshmi P, Natarajan E. Investigation of performance parameters of different photovoltaic cell materials using the lambert-w function. Energy Procedia 2016;90:566–73.

[20] Gao X, Cui Y, Hu J, Xu G, Yu Y. Lambert w-function based exact representation for double diode model of solar cells: comparison on fitness and parameter extraction. Energy Convers Manage 2016;127:443–60.

[21] Lun S-X, Du C-J, Guo T-T, Wang S, Sang J-S, Li J-P. A new explicit iv model of a solar cell based on taylors series expansion. Sol Energy 2013;94:221–32.

[22] Bogning Dongue S, Njomo D, Ebengai L. An improved nonlinear five-point model for photovoltaic modules. Int J Photoenergy 2013;2013:11.

[23] Hejri M, Mokhtari H, Azizian MR, Ghandhari M, Sder L. On the parameter extraction of a five-parameter double-diode model of photovoltaic cells and modules. IEEE J Photovoltaics 2014;4:915–23.

[24] Laudani A, Riganti Fulginei F, Salvini A. High performing extraction procedure for the one-diode model of a photovoltaic panel from experimental iv curves by using reduced forms. Sol Energy 2014;103:316–26.

[25] Mares O, Paulescu M, Badescu V. A simple but accurate procedure for solving the five-parameter model. Energy Convers Manage 2015;105:139–48.

[26] Bonkoungou D, Koalaga Z, Njomo D, Zougmore F. An improved numerical approach for photovoltaic module parameters acquisition based on single-diode model. Int J Curr Eng Technol 2015;5:3735–42.

[27] Mafarja M, Aljarah I, Heidari AA, Hammouri AI, Faris H, AlaM A-Z, et al. Evolutionary population dynamics and grasshopper optimization approaches for feature selection problems. Knowl-Based Syst 2018;145:25–45.

[28] Faris H, Al-Zoubi AM, Heidari AA, Aljarah I, Mafarja M, Hassonah MA, et al. An intelligent system for spam detection and identification of the most relevant features based on evolutionary random weight networks. Inform Fusion 2019;48:67–83.

[29] Mafarja M, Aljarah I, Heidari AA, Faris H, Fournier-Viger P, Li X, et al. Binary dragonfly optimization for feature selection using time-varying transfer functions. Knowl-Based Syst 2018.

[30] Jordehi AR. Time varying acceleration coefficients particle swarm optimisation (tvacpso): a new optimisation algorithm for estimating parameters of pv cells and modules. Energy Convers Manage 2016;129:262–74.

[31] Dizqah AM, Maheri A, Busawon K. An accurate method for the pv model identification based on a genetic algorithm and the interior-point method. Renew Energy 2014;72:212–22.

[32] Rezaee Jordehi A. Enhanced leader particle swarm optimisation (elpso): an efficient algorithm for parameter estimation of photovoltaic (pv) cells and modules. Sol Energy 2018;159:78–87.

[33] Xiong G, Zhang J, Shi D, He Y. Parameter extraction of solar photovoltaic models using an improved whale optimization algorithm. Energy Convers Manage 2018;174:388–405.

[34] Wu Z, Yu D, Kang X. Parameter identification of photovoltaic cell model based on improved ant lion optimizer. Energy Convers Manage 2017;151:107–15.

[35] Yuan X, Xiang Y, He Y. Parameter extraction of solar cell models using mutative-scale parallel chaos optimization algorithm. Sol Energy 2014;108:238–51.

[36] Mirjalili S, Gandomi AH, Mirjalili SZ, Saremi S, Faris H, Mirjalili SM. Salp swarm algorithm: a bio-inspired optimizer for engineering design problems. Adv Eng Softw 2017;114:163–91.

[37] Zhao H, Huang G, Yan N. Forecasting energy-related CO_2 emissions employing a novel ssa-lssvm model: considering structural factors in china. Energies 2018;11.

[38] Faris H, Mafarja MM, Heidari AA, Aljarah I, AlaM A-Z, Mirjalili S, et al. An efficient binary salp swarm algorithm with crossover scheme for feature selection problems. Knowl-Based Syst 2018;154:43–67.

[39] Aljarah I, Mafarja M, Heidari AA, Faris H, Zhang Y, Mirjalili S. Asynchronous accelerating multi-leader salp chains for feature selection. Appl Soft Comput 2018;71:964–79.

[40] Hussien AG, Hassanien AE, Houssein EH. Swarming behaviour of salps algorithm for predicting chemical compound activities. Intelligent computing and information systems (ICICIS), 2017 eighth international conference on. IEEE; 2017. p. 315–20.

[41] Ekinci S, Hekimoglu B. Parameter optimization of power system stabilizer via salp swarm algorithm. 2018 5th international conference on electrical and electronic engineering (ICEEE). IEEE; 2018. p. 143–7.

[42] Mohapatra TK, Sahu BK. Design and implementation of ssa based fractional order pid controller for automatic generation control of a multi-area, multi-source interconnected power system. Technologies for smart-city energy security and power (ICSESP). IEEE; 2018. p. 1–6.

[43] Asaithambi S, Rajappa M. Swarm intelligence-based approach for optimal design of cmos differential amplifier and comparator circuit using a hybrid salp swarm algorithm. Rev Sci Instrum 2018;89:054702.

[44] El-Fergany AA. Extracting optimal parameters of pem fuel cells using salp swarm optimizer. Renew Energy 2018;119:641–8.

[45] Baygi SMH, Karsaz A, Elahi A. A hybrid optimal pid-fuzzy control design for seismic exited structural system against earthquake: a salp swarm algorithm. In: Fuzzy and intelligent systems (CFIS). 2018 6th Iranian joint congress on. IEEE. p. 220–5.

[46] Rashedi E, Nezamabadi-Pour H, Saryazdi S. Gsa: a gravitational search algorithm. Inform Sci 2009;179:2232–48.

[47] Mirjalili S. Sca: a sine cosine algorithm for solving optimization problems. Knowl-Based Syst 2016;96:120–33.

[48] Li MD, Zhao H, Weng XW, Han T. A novel nature-inspired algorithm for optimization: virus colony search. Adv Eng Softw 2016;92:65–88.

[49] Mirjalili S, Lewis A. The whale optimization algorithm. Adv Eng Softw 2016;95:51–67.

[50] Mirjalili S. The ant lion optimizer. Adv Eng Softw 2015;83:80–98.